

Cu/Mg-composites: processing, structure and properties

A. Y. Volkov[†], D. A. Komkova, A. A. Kalonov

[†]volkov@imp.uran.ru

M. N. Miheev Institute of Metal Physics UB RAS, 18 S. Kovalevskaya St., Yekaterinburg, 620108, Russia

The copper-based alloys with high strength and low electrical resistivity are of interest for many practical applications. In this study, Cu/Mg-composites with 1, 7 and 49 magnesium filaments in Cu-matrix have been obtained by hydroextrusion at room temperature. The structure, mechanical and electrical properties of the composite rods and thin wires in the deformed and annealed states have been investigated. The strength of the deformed Cu/Mg-composite with a minimal volume fraction of magnesium was found to be abnormally high. The increase of magnesium microhardness was revealed to be near the interface. A change in the lattice constant of the Cu-matrix in the deformed Cu/Mg-composites is discovered by the XRD-method. It has been concluded that, under severe plastic deformation, different solid solutions form on the Cu/Mg-interfaces due to mechanical alloying processes. The Cu/Mg-composite with a maximal volume fraction of Mg has the lowest strength in the deformed state, however, it becomes the strongest one after annealing at 200°C due to annealing hardening of magnesium. The temperature dependences of the electrical resistivity of Cu/Mg-composites differ significantly from each other. During heating, three eutectic transformations are realized in the composite with 7 Mg-filaments. As a result, the electrical resistivity of the deformed Cu/7Mg-composite increases almost two times. The specific electrical resistivity of the composite with 49 Mg-filaments is a bit different from the electrical resistivity of deformed copper. The mechanisms of structure formation during the heating of these composites have been shown to be significantly different. The obtained results can be used for the development of high-strength Cu-based conductors.

Keywords: bimetallic composite, Cu/Mg diffusion couple, severe plastic deformation, mechanical properties, electrical conductivity.

1. Introduction

In the last decades, growing attention has been focused on the development of copper-based alloys with high strength and good electrical conductivity [1]. In recent times, there have been appearing more and more works investigating the structures and properties of conductive materials based on the Cu-Mg alloys strengthened by different SPD-methods [1–3]. According to [3], contact wires of the Cu-Mg alloys have great potential for commercial application, for example, to satisfy the needs of the high-speed electrical railways.

In contrast to a large number of works on Cu-Mg-alloys, studies on Cu/Mg-composites are not so numerous. Probably, the main reason that prevents the researchers from working on the development of Cu/Mg-composites is related to doubts on the possibility of reinforcing copper matrix by Mg-filaments. At present, researchers have tried to reinforce Cu by adding metallic fibers or nanoparticles (Nb, Cr, Zr, etc) [4,5], ceramic particles (Al₂O₃, ZnO, TiB₂, etc.) [6] and carbon fibers [7]. Nevertheless, producing Cu/Mg-composites may be a new way in order to develop high-strength materials with a low electrical resistivity.

The purposes of this study were to develop a technique for fabrication of Cu/Mg-composites with various numbers of Mg-filaments and to reveal the effect of the deformation and heat treatment on the microstructure, electrical and mechanical properties of these composites.

2. Materials and methods

According to [1–3], a variation of the Cu/Mg-ratio will lead to a change in the phase composition, microstructure and properties of the Cu/Mg-alloys. Therefore, at the first stage of the research, it is necessary to understand the influence of the volume fraction, number and diameter of Mg-filaments on the structure and properties of the Cu/Mg-composites. In this study, there were obtained and investigated composite rods and wires, which contained 1, 7 and 49 Mg-filaments inside the Cu-matrix. Further, we will indicate the numbers of magnesium filaments in the designations of composites. For example, a composite containing 1 Mg-core in Cu-sleeve will be noted as follows: Cu/1Mg-composite.

At the first step, we placed a magnesium workpiece of 12 mm in diameter in a Cu-container of 18 mm in diameter. To obtain a Cu/1Mg-composite, this “assembly” was hydrostatically extruded at room temperature through a die of 10 mm in diameter. To fabricate a Cu/7Mg-composite rod, the Cu-container of 18 mm in diameter with 7 holes having diameters of 3 mm was used. 7 rods of the Cu/1Mg-composite of 3 mm in diameter were tightly inserted into these holes. Then, this Cu-Mg assembly was consecutively subjected to hydroextrusion at room temperature through dies with diameters of 10, 6, and 3 mm. Fig. 1 shows the views of the as-extruded rods of the Cu/1Mg-composite (a) and Cu/7Mg-composite (b) 6 mm in diameter. The fabrication process of the Cu/49Mg-composite is the same as it was

described above for the Cu/7Mg-composite. However, in this case, the Cu-container with 7 holes was merged with 7 rods of the Cu/7Mg-composite. Finally, the extruded 3-mm rods of Cu/1Mg, Cu/7Mg and Cu/49Mg composites were drawn into thin wires.

Before the hydroextrusion, all Cu-containers, Mg-workpiece and composite rods of 3 mm in diameter were preliminarily annealed at 200°C for 3 hours. It is known that two kinds of intermetallic compounds (Cu_2Mg and CuMg_2) may be formed during the heating of the Cu/Mg diffusion couples [8]. The CuMg_2 phase layer appears at approximately 215°C, followed by the formation of the Cu_2Mg phase at about 380°C in the presence of excess Cu. It may be concluded, that annealing at 200°C would not lead to the formation of new phases at the Cu/Mg interface. However, such thermal treatment causes the recrystallization of copper [9].

The electrical resistivity of the samples of 0.25 mm in diameter was measured by the four-probe technique at a direct current of 20 mA. The absolute deviation of the electrical resistivity measurements was found to be $\Delta\rho = \pm 0.04 \times 10^{-8} \Omega\text{m}$ [10]. The strength properties of the composite wire of 1.5 mm in diameter and 30 mm in length were measured by tensile testing using an Instron 5982 test machine with the strain rate equal to 3 mm/min. Vickers microhardness values were determined using a PMT-3 tester with 0.02 kg load and dwelling time of 30 s. Each microhardness datum is the average value of at least 10 measurements. A QUANTA 200 FEI scanning electronic microscope was used to characterize the microstructure of the composites. X-ray diffraction (XRD) analysis was performed using a Rigaku DMAX 2200 diffractometer by the method of continuous recording at a speed of 4°. $\text{Cu}_{\text{K}\alpha}$ radiation was monochromatized with a graphite single crystal.

The accumulated deformation strain is defined by the known equation: $e = \ln(S_0/S_f)$, where S_0 and S_f are the initial and final cross-section areas of Mg-filaments, respectively.

3. Results

3.1. Compositions and structures of the Cu/Mg-composites under investigation

Fig. 1 shows the views of the as-extruded rods of the Cu/1Mg-composite (a), Cu/7Mg-composite (b) 6 mm in diameter and Cu/49Mg-composite rods of 4 mm in diameter.

Based on these pictures, we estimated the volume fractions of copper and magnesium in our composites (Table 1). The Cu and Mg contents in weight and atomic percent may be calculated in each of the studied composites using their volume fractions.

Table 1. The Cu/Mg-ratio in the obtained composites.

Composite	Volume fraction, %		Wt. %		At. %	
	Cu	Mg	Cu	Mg	Cu	Mg
Cu/1Mg	55.5	44.5	86.4	13.6	70.9	29.1
Cu/7Mg	91.4	8.6	98.2	1.8	95.3	4.7
Cu/49Mg	98.4	1.6	99.7	0.3	99.2	0.8

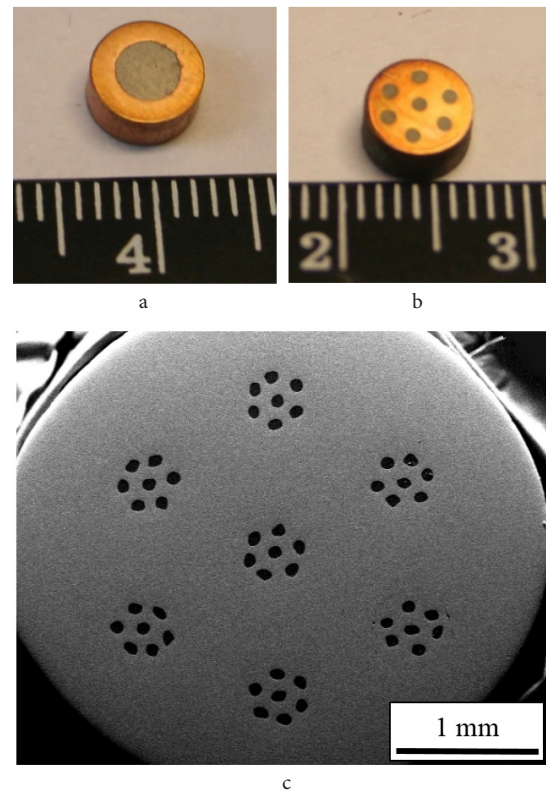


Fig. 1. (Color online) Cross-sections of the Cu/1Mg-composite (a), Cu/7Mg-composite (b), Cu/49Mg-composite (c) rods.

3.2. Resistometric study of the Cu/Mg-composites

3.2.1. Electrical resistivity of the as-extruded composites

After the hydroextrusion and drawing with the accumulated strain $e \approx 6.0$, the specific electrical resistivity of copper is $\rho_{\text{Cu}} = 1.83 \times 10^{-8} \Omega\text{m}$. To determine the resistivity of deformed magnesium, the deformed Cu/1Mg-composite rod was taken and the Cu-sleeve was removed from it. The electrical resistivity of the deformed Mg-core ($e \approx 3.3$) is $\rho_{\text{Mg}} = 4.85 \times 10^{-8} \Omega\text{m}$.

The results of the resistometric study of the Cu/Mg-composites under investigation are listed in Table 2. The specific electrical resistivity of the deformed Cu/1Mg-composite is $\rho_{\text{Cu/1Mg}} \approx 2.35 \times 10^{-8} \Omega\text{m}$. It regularly drops to $\rho_{\text{Cu/7Mg}} \approx 2.07 \times 10^{-8} \Omega\text{m}$ in the Cu/7Mg-composite due to an increased content of copper. The content of copper in the Cu/49Mg-composite is the highest. As a result, its specific electrical resistivity ($\rho_{\text{Cu/49Mg}} \approx 1.88 \times 10^{-8} \Omega\text{m}$) is the lowest of all the investigated samples. It is clearly seen, the value of the resistivity of the Cu/49Mg-composite is only slightly higher compared with the deformed copper.

Table 2. Electrical resistivity and yield stress of the deformed Cu, Mg and Cu/Mg-composites.

	Specific electrical resistivity, ρ , $10^{-8} \Omega\text{m}$	Yield stress, $\sigma_{0.2}$, MPa
Cu	1.83	350
Mg	4.85	97
Cu/1Mg	2.35	290
Cu/7Mg	2.07	322
Cu/49Mg	1.88	386

3.2.2. Temperature dependences of electrical resistivity

Fig. 2 and Fig. 3 show the temperature dependences of the electrical resistivity obtained at heating (curves 1) and cooling (curves 2) of the deformed Cu/7Mg-composite and Cu/49Mg-composite, respectively. These figures also show the temperature derivatives of the electrical resistivity versus the temperature, dp/dT (curves 3), which are plotted only for the stage of heating (i.e. they correspond to curves 1).

Three stages of the rapid resistivity growth at the heating of the Cu/7Mg-composite are clearly visible in curve 1 in Fig. 2. Each of these stages is a response to the eutectic transformations in the phase diagram at $\sim 490^\circ\text{C}$, $\sim 560^\circ\text{C}$ and $\sim 730^\circ\text{C}$ [11]. It can be assumed, a significant amount of intermetallic phases Cu_2Mg and/or CuMg_2 with low electrical conductivity are formed at the Cu/Mg-interfaces. Therefore, after cooling to room temperature, the electrical resistivity of the initially deformed Cu/7Mg-composite increases almost two times.

Fig. 3 shows the results of the resistometric study obtained at the heating and cooling of the Cu/49Mg-composite. This temperature dependence of the resistivity obtained during heating (curve 1) does not have sharp visual changes. Moreover, when heated to 550°C , the dependence is almost linear. With further heating, electrical resistivity grows some faster. A very wide peak on the dp/dT plot corresponds to this region, the peak maximum being at $\sim 730^\circ\text{C}$ (curve 3). In addition, a very slight difference is in the resistivity values of the Cu/49Mg-composite before and after the experiment with the heating of the sample to 750°C followed by cooling.

3.3. Mechanical properties of the Cu/Mg-composites

The results of the mechanical tests of the extruded samples of Cu, Mg and Cu/Mg-composites are shown in Table 2. The yield stress of the Cu/1Mg-composite is 290 MPa. It has the lowest mechanical properties. The experimental yield stress of the Cu/7Mg-composite is 322 MPa. We believed the yield stress of the Cu/49Mg-composite should be slightly lower than that of copper. However, the yield stress

of the Cu/49Mg-composite was 386 MPa and significantly exceeded the yield stress of extruded copper.

Annealing at 200°C for 3 hours leads to the regular decrease in the mechanical properties of all the investigated samples. For example, the yield stress of the annealed copper (73 MPa) is 1/5 that for the deformed copper (350 MPa). Unlike copper, annealing of the deformed magnesium at a temperature of 200°C leads to an increase in its yield stress: from 97 MPa to 127 MPa [12]. It is quite interesting, however, the strength of annealed Mg is higher compared with annealed Cu. The Cu/1Mg-composite has the highest magnesium content. Therefore, this composite, which had the lowest strength in the deformed state, became the strongest of all investigated composites after the annealing ($\sigma_{0.2}=100$ MPa). Note that the annealing significantly increases the plastic properties of the investigated composites.

The obtained results confirmed that the annealing temperature we chose (200°C) was suitable for the plasticization of the deformed workpieces before the hydroextrusion.

3.4. Microhardness and the element distribution at the Cu/Mg-interfaces

According to the results of the mechanical tests, the strength of the deformed Mg is low. Really, a strong decrease of microhardness value is observed in the extruded Cu/7Mg-composite upon the transition from the Cu-matrix to the Mg-filament. In contrast, the microhardness of Mg-filament near the interface in the Cu/49Mg-composite is abnormally high (Fig. 4). To understand the reason for these differences, the element distribution was analysed at the interface of the Cu/49Mg-composite.

According to Fig. 5, there is a diffusion of Cu-atoms into the Mg-filament. The thickness of the mixed Cu-Mg layer at the interface of the Cu/49Mg-composite may be estimated at about $10\text{ }\mu\text{m}$.

As a whole, the microhardness measurement results in Fig. 4 are in good agreement with the element distribution at the interface of the Cu/49Mg-composite (Fig. 5). Really,

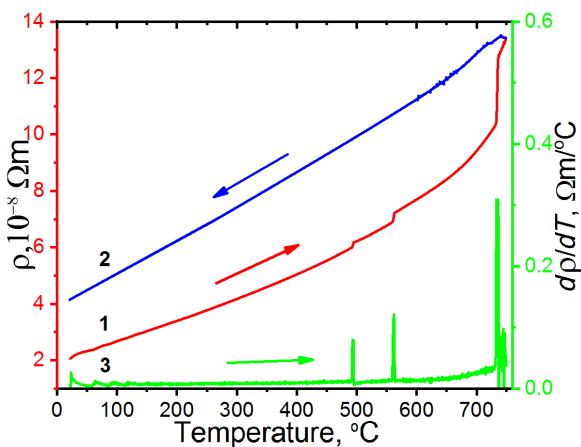


Fig. 2. (Color online) Resistometric study results of the Cu/7Mg-composite: temperature dependences of the electrical resistivity obtained during the heating (curve 1) and cooling (2) and the temperature derivative (3), which corresponds to curve 1. The heating and cooling rate is 120 degrees/hour.

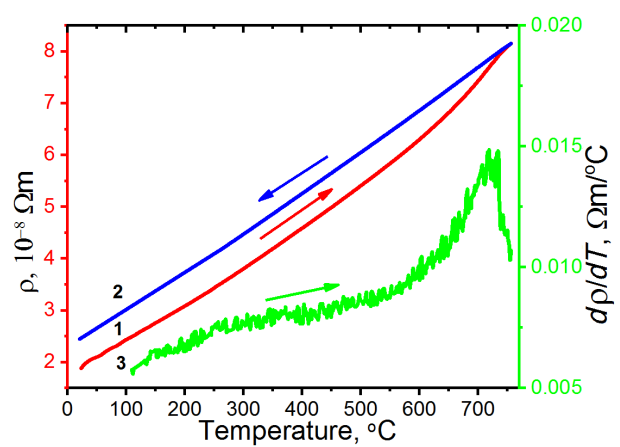


Fig. 3. (Color online) Resistometric study results of the Cu/49Mg-composite: temperature dependences of the electrical resistivity obtained during the heating (curve 1) and cooling (2) and the temperature derivative (3), which corresponds to curve 1. The heating and cooling rate is 120 degrees/hour.

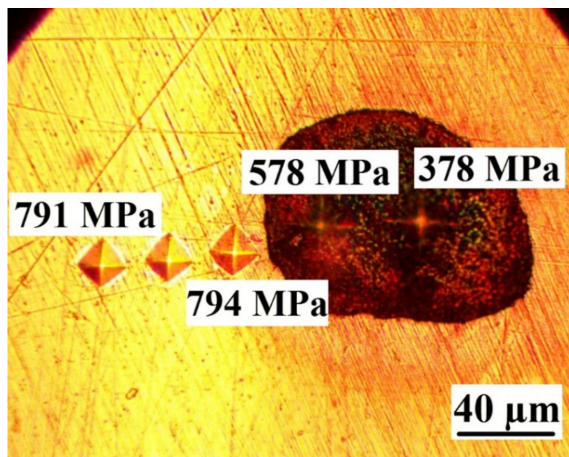


Fig. 4. (Color online) Microhardness measurements across the Cu/Mg-interface in the deformed Cu/49Mg-composite.

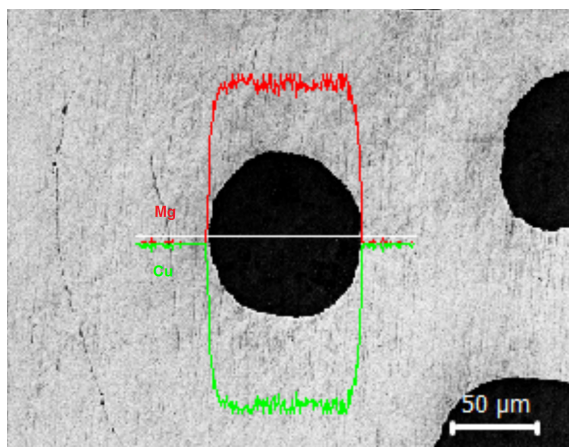


Fig. 5. (Color online) Distribution of elements along the line crossing the Mg-filament in the Cu/49Mg-composite.

any solid solution has more high strength than its constituent metals have [2].

It can be assumed, that the mixing of Cu and Mg atoms will be continued under SPD during making the thin wire from the composite rod. However, it is very difficult to obtain an XRD-diffractogram from the thin wires. Therefore, the pack of the thin deformed Cu/7Mg-composite wires with 0.25 mm in diameter was made for the experiment in Fig. 6.

In Fig. 6, the X-ray diffraction pattern of pure Cu is superimposed on the XRD pattern, obtained from the center of this pack. It is well seen, the Cu-peak changes its position towards higher angles. It means that the lattice constant of Cu is decreased under SPD of the Cu/Mg-composites due to the formation of the Cu-based solid solution.

4. Discussion

To clarify the features of the property formation of the Cu/Mg-composites under investigation, the structural transformations on their interfaces have to be studied in details. The work in this direction has already started [13]. However, it seems that the results obtained in this work

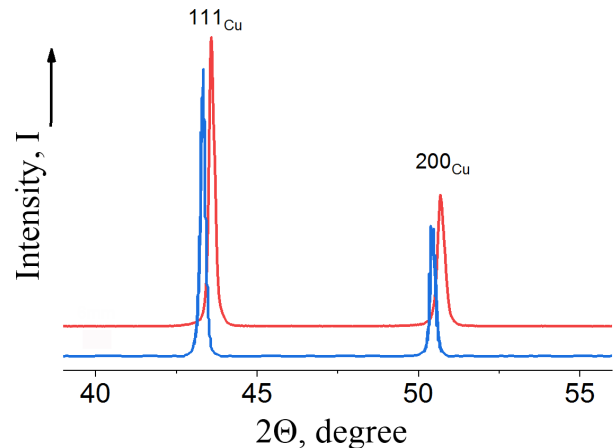


Fig. 6. (Color online) XRD-spectra of the as-extruded pure Cu (blue curve) and the pack of the thin Cu/7Mg-composite wires (red curve) after SPD with accumulated deformation strain $\epsilon \approx 12.1$.

in combination with literature data are sufficient to understand the processes that occur in the composites under investigation.

The conclusion may be made from the microhardness results (Fig. 4), that the solid solution of Cu in Mg is forming in the surface of the Mg-filaments of the Cu/49Mg-composite. As it was found before [11], the diffusion rate of Cu-atoms into Mg is much higher than that in the opposite direction. The strength of the solid solution is greater than that of each of its components. As a result, the microhardness of Mg-filament increases near the interfaces in the thick rod of the Cu/49Mg-composite. It may be concluded, that the Mg-based solid solution forms in the Cu/Mg-interface at the first stage of SPD (Fig. 5). In turn, at the high level of SPD, the supersaturated Cu-based solid solution is formed in the deformed thin wire of the Cu/49Mg-composite instead of 49 Mg-filaments (Fig. 6). It is due to the exhaustion of Mg-sources in the Cu-matrix. The result of the resistometric study in Fig. 2 confirms this conclusion.

As it was revealed in [16], the CuMg_2 intermetallic layer in Cu/Mg super-laminates composites can grow with a sufficient growth rate at low temperatures (less than 200°C). However, there are no reports in the literature on the accelerated diffusion of magnesium into copper (and vice versa) at room-temperature SPD of the Cu/Mg-couple.

In general, a gradient of chemical potential across the interface, a strong surface curvature of the fine filaments, a high level of the stored elastic energy, and a high concentration of defects during SPD can lead to an increase in the diffusion rate [15]. The discussed phenomenon is very reminiscent of mechanical alloying (MA) processes. The result of the MA processes can be non-equilibrium phases including supersaturated solid solutions, metastable crystalline and quasi-crystalline phases, nanostructures, and amorphous alloys. It was found [16] that MA processes could be realized if severe deformation and shear strains are simultaneously applied to the sample.

We suppose that strong shear strains arise in the fabrication process of Cu/Mg-composites. Indeed, it was observed that the copper sleeve was flowing faster than

the magnesium core during the cold hydroextrusion of the composites. This phenomenon can be explained by the difference in the deformation mechanisms of Cu with its face-centered cubic crystalline structure and Mg, which has the hexagonal close-packed lattice. Deformation strains attained during the hydroextrusion are also very high. For example, the accumulated deformation strain in the Cu/49Mg-composite wire of diameter 0.25 mm for the resistometric study is $\epsilon \approx 5.6$. Such a high level of deformation strain is comparable with the one realized at the high-pressure torsion (HPT) deformation method [16,17].

Very large deformation and shear strains can lead to the synthesis of non-equilibrium phases [16]. For example, HPT of Ag and Cu powders allowed obtaining a solid solution with Ag-content of $\sim 30\%$ [17]. Such a solid solution is extremely non-equilibrium one and degrades at heating. Similar experiments carried out on a mixture of Cu and Nb also resulted in the formation of non-equilibrium Nb-enriched segregation zones or Nb-rich secondary precipitates [18]. Based on these results, one may believe that a new non-equilibrium Cu-Mg-phase (or a set of different phases) is formed in the thin wire of the deformed Cu/Mg-composite instead of Mg-filaments.

For example, Cu-based solid solutions with different contents of solute elements were many times investigated before by resistometric methods [2,8,19]. It is established that the temperature dependence of the electrical resistivity of such alloys has a linear form. The low-temperature part of curve 1 in Fig. 3 also has a linear form but the plot of the corresponding temperature derivative helps to reveal two features (curve 3 in Fig. 3). Firstly, a small but obvious change of inclination of the dp/dT dependence near 300°C points to some transformation within this temperature interval. Secondly, within the high-temperature area of this temperature dependence, there is observed a wide peak, the maximum of which is at $\sim 730^\circ\text{C}$. This temperature coincides completely with the temperature of the eutectic reaction between the Cu_2Mg intermetallic compound and Cu-based solid solution [11]. Obviously, the particles of the Cu_2Mg phase originated in the Cu/49Mg-composite during our experiment.

Moreover, in SPD-materials the temperature of the new phase formation onset may significantly decrease. For example, the CuMg_2 phase arises in the Cu/Mg diffusion couple at 215°C [11] but in deformed Cu/Mg super-laminate composites the particles of this phase grow with a sufficient rate at temperatures below 200°C [14]. We believe that the change of the dp/dT plot inclination near 300°C (curve 3 in Fig. 3) is related to the precipitation processes of the Cu_2Mg phase from the supersaturated solid solution.

Based on our results (see Fig. 3 and Fig. 6), the conclusion can be made that 49 fibers of the supersaturated Cu-based solid solution were formed in the deformed thin wire of the Cu/49Mg-composite instead of 49 Mg-filaments. It allows explaining the high mechanical properties of the deformed Cu/49Mg-composite. The resistivity of the Cu/49Mg-composite is just a little different from the specific electrical resistivity of the copper (Table 2). It is due to the copper matrix makes up the bulk of the Cu/49Mg-composite. As a result, the deformed

Cu/49Mg-composite has a good combination of high strength and low electrical resistivity.

It is interesting that the Cu/49Mg-composite becomes less strong after annealing. On the contrary, the Cu/1Mg-composite, which was the weakest one in the deformed state, became the strongest of all the investigated composites after annealing. Such an unusual change of the mechanical properties of the Cu/Mg-composites is well explained by the phenomenon of a thermal anomaly of magnesium strength. It has been shown in our works [12,20] that low-temperature treatments lead to an increase in the yield stress of pre-deformed magnesium. The plasticity of magnesium does not change after such annealing. We believe, that the abnormal annealing hardening of pure magnesium can be explained by the thermally activated processes of rearrangement of the dislocation structure and self-blocking of a part of the dislocations [12]. The Cu/1Mg-composite contains the largest amount of magnesium and, therefore, after annealing at 200°C it becomes the strongest one due to the annealing hardening phenomenon of pure magnesium. A similar result was obtained before in the investigation of Al/Mg/Al laminates, which exhibited the best mechanical properties after annealing at 200°C for 1–4 hours [21].

Thus, our hypothesis about the formation of some volume of the supersaturated Cu (Mg) solid solution at the Cu/Mg-interfaces explains the abnormally high strength and low electrical resistivity of the severely deformed Cu/49Mg-composite rather well.

Conclusions

The paper shows that SPD by hydroextrusion followed by drawing leads to sufficiently high mechanical properties of the Cu/Mg-composite, which contains 49 Mg-filaments. The electrical resistivity of such an SPD material is only slightly higher than the electrical resistivity of copper. To explain the observed phenomena, we put forward an assumption about the formation of some volume of supersaturated solid solution in the deformed Cu/Mg-composites. This is caused by a very large deformation and shear strains, which arise in the process of making our composites and can lead to MA processes at the Cu/Mg-interface. If this hypothesis is correct, then a significant increase in the number of thin Mg-filaments will make it possible to increase significantly the mechanical properties of the deformed Cu/Mg-composite without a noticeable increase in the electrical resistivity. We have already begun working in this direction and obtained a Cu/Mg-composite, which contains about one million fine magnesium filaments.

Thus, the results of the study are of interest in terms of developing new technologies for producing high-strength metal composites.

Acknowledgments. The work was carried out in the framework of a state task according to the theme "Pressure" No. AAAA-A18-118020190104-3. The studies of structure and mechanical properties of the samples were carried out at the Electron Microscopy Department and Mechanical Test Department of the Collective-Use Center of the Institute of Metal Physics (Ural Branch, Russian Academy of Sciences).

References

1. S. Gorsee, B. Ouyard, M. Goune, A. Poulon-Quintin. *J. Alloys Comp.* 633, 42 (2015). [Crossref](#)
2. K. Maki, Yu. Ito, H. Matsunaga, H. Mori. *Scripta Mater.* 68, 777 (2013). [Crossref](#)
3. Ch. Zhu, A. Ma, J. Jiang, X. Li, D. Song, D. Yang, Yu. Yuan, J. Chen. *J. Alloys Comp.* 582, 135 (2014). [Crossref](#)
4. L. Deng, K. Han, K. T. Hartwing, T. M. Siegrist, L. Dong, Z. Sun, X. Yang, Q. Liu. *J. Alloys Comp.* 602, 331 (2014). [Crossref](#)
5. I. V. Khomskaya, V. I. Zeldovich, A. V. Makarov, A. E. Kheifets, N. Y. Frolova, E. V. Shorochoy. *Lett. Mat.* 3, 150 (2013). (in Russian) [Crossref](#)
6. Yu. Qi, A. Kosinova, A. R. Kilmametov, B. B. Straumal, Eu. Rabkin. *Mater. Charact.* 145, 389 (2018). [Crossref](#)
7. Z. Huang, Zh. Zheng, Sh. Zhao, Sh. Dong, P. Luo, L. Chen. *Mater. Des.* 133, 570 (2017). [Crossref](#)
8. B. Arcot, S. P. Murarka, L. A. Clevenger, Q. Z. Hong, W. Ziegler, J. M. E. Harper. *J. Appl. Phys.* 76 (9), 5161 (1994). [Crossref](#)
9. A. Yu. Volkov, O. S. Novikova, A. E. Kostina, B. D. Antonov. *Phys. Met. Metallogr.* 117 (9), 945 (2016). [Crossref](#)
10. A. Yu. Volkov, O. S. Novikova, B. D. Antonov. *J. Alloys Comp.* 581, 625 (2013). [Crossref](#)
11. K. Nonaka, T. Sakazawa, H. Nakajima. *Mater. Trans., JIM.* 12, 1463 (1995). [Crossref](#)
12. A. Yu. Volkov, I. V. Kliukin. *Mater. Sci. Eng. A.* 627, 56 (2015). [Crossref](#)
13. A. Yu. Volkov, A. A. Kalonov, D. A. Komkova, A. V. Glukhov. *Phys. Met. Metallogr.* 119 (10), 946 (2018). [Crossref](#)
14. K. Tanaka, D. Nishino, K. Hayashi, S. Ikeuchi, R. Kondo, H. T. Takeshita. *Int. J. Hydrogen Energy.* 42, 22502 (2017). [Crossref](#)
15. K. Wongpreedee, A. M. Russel. *Gold Bull.* 40 (3), 199 (2007). [Crossref](#)
16. C. Suryanarayana. *Progr. In Mater. Sci.* 46, 1 (2001). [Crossref](#)
17. T. Tolmachev, V. Pilyugin, A. Ancharov, A. Patselov, E. Chernshev, K. Zolotarev. *Phys. Proc.* 84, 349 (2016). [Crossref](#)
18. M. Kapoor, T. Kaub, K. A. Darling, B. L. Boyce, G. B. Thompson. *Acta Mat.* 126, 564 (2017). [Crossref](#)
19. J. Freudenberg, A. Kauffmann, H. Klaub, T. Marr, K. Nevkov, V. Subramanya Sarma, L. Schultz. *Acta Mater.* 58, 2324 (2010). [Crossref](#)
20. D. A. Komkova, A. Yu. Volkov. *Met. Sci. Heat Treat.* 59 (11-12), 755 (2018). [Crossref](#)
21. H. Nie, W. Liang, H. Chen, L. Zheng, Ch. Chi, X. Li. *Mater. Sci. Eng. A.* 732, 6 (2018). [Crossref](#)